On the use of Magnetically Coupled Resonant Snubbers to Mitigate the Electromagnetic Emission of Power Switching Circuits

On the Use of Magnetically Coupled Resonant Snubbers to Mitigate the Electromagnetic Emission of Power Switching Circuits

Franco Fiori, *Member, IEEE*

***Abstract*—This letter presents a novel solution to attenuate the electromagnetic emission of power switching circuits due to the resonance of the loop parasitic inductances with the parasitic capacitances of the power devices. A resonant snubber based on the magnetic coupling of a power parasitic loop causing unwanted oscillations with another one inserted at the printed circuit board level purposely and loaded by a dissipative element, is presented. A design method is proposed and used to damp the unwanted oscillations affecting the switching voltage and current in a prototype, which was specifically designed and fabricated to validate the proposed solution. The conducted emission delivered by such a prototype equipped with the resonant snubber, with an RC snubber and without any snubber are compared.**

***Index Terms*—Electromagnetic emission, snubber, power electronics, resonant transformer.**

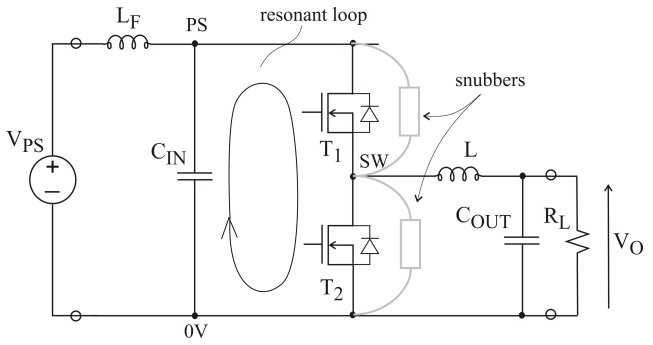

Fig. 1. Concept schematic view of a DC-DC Buck converter.

I. Introduction

The continuous reduction of the power transistors switching time has made possible the design of high voltage power modules featuring higher conversion efficiency and smaller cooling systems. However, the use of faster power devices has increased the level of electromagnetic emission at high frequencies [1], which can be confined to the power module itself with filters and shields [2] or attenuated using software-based solutions such as the spread spectrum technique [3] or the delay compensation technique [4]. Alternatively, the switching noise can be mitigated at the root by inserting snubbers in the power circuit. Such auxiliary circuits reduce the electromagnetic emission by lowering the slope of the switching voltages (currents). Actually, they are largely used to reduce the voltage (current) stress of power transistors (commutation spikes) as well as to lower the switching losses, since they modify the switching trajectory of the power devices [5]. Usually, they are classified as active and passive. The former are based on active switches driven in a synchronous fashion with the power transistors and reactive components [6], the latter are based on passive components and diodes and are usually divided into lossless and lossy (RC or RL snubbers) depending on their capability to recover the switching energy [7]. However, as far as hard switching circuits are concerned and switching losses are lowered exploiting the full switching speed of fast transistors, unwanted oscillations are usually experienced [8]. For instance, in the Buck converter shown in Fig. 1, the fast turn-on of T_2 (T_1) excites the stray inductance of the switching loop $C_{\rm IN}$, T_1, T_2 and the parasitic capacitance of the switched off transistor T_1 (T_2), i.e., $C_{\rm DS-1}$ ($C_{\rm DS-2}$) causing high frequency oscillations, which can be damped using lossy snubbers [9].

This letter proposes a magnetically coupled resonant snubber, which affects the switching waveforms at high frequency only, just around the frequency band of interest, thus lowering the electromagnetic emission but affecting the conversion efficiency of the switching circuit negligibly.

The letter is organized as follows. Section II presents the resonant transformer composed of the parasitic power loop and another loop added in the circuit purposely to damp the oscillations. Section III shows the experimental validation of the proposed solution and some concluding remarks are drawn in Sec. IV.

The author is with the Department of Electronics and Telecommunications, Politecnico di Torino, Torino I-10129, Italy. (e-mail: franco.fiori@polito.it)

II. Magnetically Coupled Resonant Snubber

As far as passive lossy snubbers are concerned, high frequency oscillations can be damped using RC or RL snubbers [5]. With RL snubbers, the parallel of the damping resistor and the snubber inductor is inserted in the power loop (T_1-T_2-$C_{\rm IN}$), and the damping resistance is effective above the snubber cut off frequency. The resonance is critically damped for

$$R_{cr-series} = 2\sqrt{\frac{L_{\rm P}}{C_{\rm DS-i}}}, \tag{1}$$

where $i = 1, 2$ depending on the switching transistor. The drawback of using RL snubber deals with the fact that a series element (e.g., a ferrite bead) is inserted in the main current path, and this lowers the reliability of the power module and increases the power loss [9], [10].

Wanting to damp the oscillations in the power loop

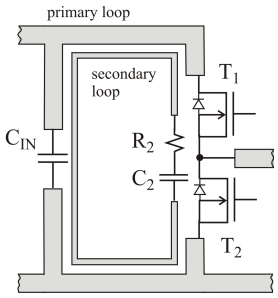

Fig. 2. Concept layout view of the resonant transformer integrated in a PCB. The secondary loop is laid out inside the primary one in order to maximize the mutual inductance.

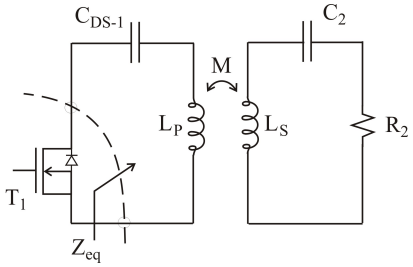

Fig. 3. Reduced schematic view of the resonant snubber highlighting the transformer (L_P, L_S, M), the parasitic capacitance $C_{\mathrm{DS}-1}$, the damping resistor R_2, and the capacitor C_2.

(T_1,T_2,C_IN), and to avoid using neither RC nor RL snubbers, the possibility to virtually include a series damping resistance in the power loop was explored. To do that, the magnetic coupling of the power loop with another one laid out nearby purposely, was exploited. In practice, once defined the layout view of the power circuit that meets the power design constraints, the power loop, i.e., the primary loop of the transformer was identified and another one (the secondary loop) is laid out as close as possible to the primary one in order to maximize the magnetic mutual coupling. An example of that is shown in Fig. 2. Furthermore, the secondary loop is loaded by C_2 and R_2 in order to build up a resonant transformer, and C_2 is chosen to tune the secondary circuit at the resonance frequency of the primary one. An equivalent circuit showing the resonant trasformer is sketched in Fig. 3. In it, L_P is the primary loop self inductance, L_S the secondary loop self inductance, M is the mutual inductance, thus the equivalent impedance seen by T_1 with T_2 switched off can be expressed as

$$Z_\mathrm{eq} = \frac{1}{sC_{\mathrm{DS}-1}} + sL_\mathrm{P} - \frac{s^3M^2}{1 + sR_2C_2 + s^2L_\mathrm{S}C_2}. \quad (2)$$

Furthermore, if $s = j\omega$, the real part and the imaginary part of Z_eq can be expressed as

$$\Re(Z_\mathrm{eq}) = \frac{\omega^4 R_2 C_2^2 M^2}{(1 - \omega^2 L_\mathrm{S} C_2 + \omega^2 (R_2 C_2)^2)}; \quad (3)$$

$$\Im(Z_\mathrm{eq}) = \frac{\omega^2 L_\mathrm{P} C_{\mathrm{DS}-1} - 1}{\omega C_{\mathrm{DS}-1}} + \frac{(1 - \omega^2 L_\mathrm{S} C_2)\omega^3 M^2 C_2}{(1 - \omega^2 L_\mathrm{S} C_2 + \omega^2 (R_2 C_2)^2)}. \quad (4)$$

For

$$C_2 = \frac{L_\mathrm{P}}{L_\mathrm{S}} C_{\mathrm{DS}-1}, \quad (5)$$

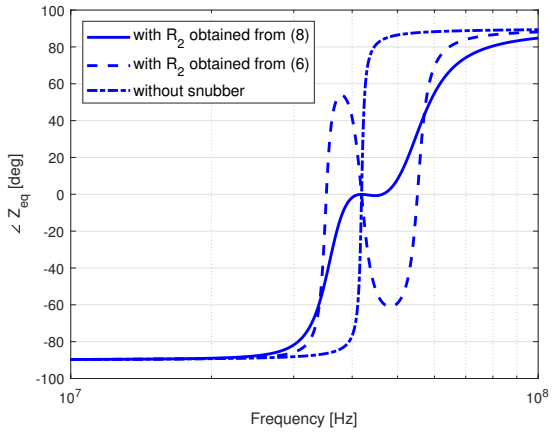

Fig. 4. Phase of Z_{eq} versus frequency obtained for $C_{\mathrm{DS}-1} = 830$ pF, $L_\mathrm{P} = 17.4$ nH, $L_\mathrm{S} = 19.5$ nH, $C_2 = 740$ pF, $M = 7.9$ nH. The continuous line was obtained with $R_2 = 2.2\ \Omega$, which in turn resulted from (8). The dashed line refers to the critically damped case $R_2 = 0.47\ \Omega$ was obtained from (6) imposing $\Re(Z_\mathrm{eq}(\omega_{r1})) = R_{\mathrm{cr-series}}$). The dash-dotted line was obtained without any snubber.

$\Im(Z_\mathrm{eq})$ is null at $\omega_{\mathrm{r}1} = (L_\mathrm{P} C_{\mathrm{DS}-1})^{-\frac{1}{2}}$ (see Eqn. (4)) and the real part can be expressed as

$$\Re(Z_\mathrm{eq}(\omega_{r1})) = \frac{\omega_{r1}^2 M^2}{R_2}. \quad (6)$$

Based on that, one could conclude that in order to critically damp the oscillations, R_2 could be derived from (6) by imposing $\Re(Z_\mathrm{eq}(\omega_{r1})) = R_{cr-series}$. In such a case, the equivalent impedance is real at ω_{r1} only but around that the impedance phase changes significantly, resulting in a poor damping of the switching noise. Aiming to obtain a resistive impedance over a larger frequency band, R_2 was calculated imposing

$$\frac{d}{d\omega}\left[\angle Z_\mathrm{eq}\right]\Big|_{\omega=\omega_{r1}} = 0. \quad (7)$$

Indeed, this equation is met for

$$R_2 = \frac{M}{\sqrt{C_2 L_\mathrm{P}}}. \quad (8)$$

Fig. 4 shows the phase of the equivalent impedance Z_eq evaluated for $R_2 \to \infty$ (dash dotted line), R_2 calculated in order to critically damp the oscillation at ω_{r1} (dashed line), R_2 obtained from (8) (continuous line) in order to damp the oscillations over a wider frequency range. The plots were obtained from (2) with $L_\mathrm{P} = 17.4$ nH, $L_\mathrm{S} = 19.5$ nH, $M = 7.9$ nH, $C_{\mathrm{DS}-1} = 830$ pF and $C_2 = 740$ pF. The transformer parameters were obtained from the measurements carried out on the prototype presented in the next Section. Actually, they can be derived before fabricating the printed circuit board (PCB) performing the electromagnetic analysis of the PCB layout with a parasitic extraction tool. $C_{\mathrm{DS}-1}$, the parasitic capacitance at the primary side can be found in the datasheet of the high side transistor or it can be obtained from the characterization of a test sample. Finally, C_2 can be calculated by (5).

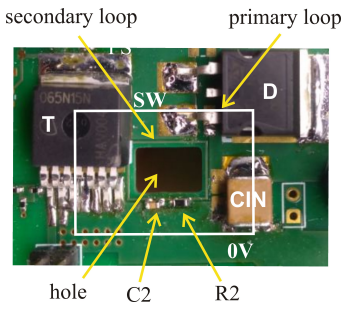

Fig. 5. Picture of the test board. Detail of the power loop including the resonant snubber.

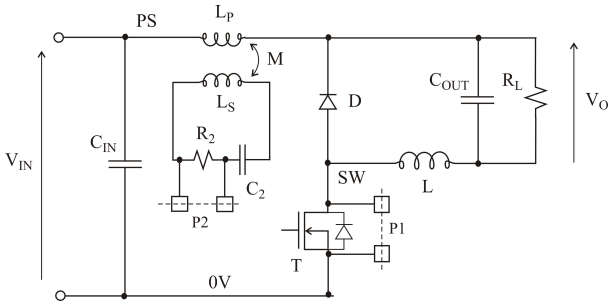

Fig. 6. Schematic view of the test circuit used in the experimental tests.

III. Experimental Results

The effectiveness of the proposed solution was checked performing conducted emission tests on the non-synchronous Buck converter shown in Fig. 6. The circuit was specifically designed and prototyped for this purpose. It is composed of the inductor $L = 220$ μH, the input capacitor $C_{\rm IN} = 2.2$ μF, the output capacitor $C_{\rm OUT} = 2.2$ μF, the transistor T (IPB065N15N3) and the free wheeling diode D (STPS40M80CG). A microcontroller (not shown in Fig. 6) drives the power section with a pulse width modulated signal, which is provided to the transistor gate-source port through a gate driver to keep the output voltage to $V_{\rm O} = 5$ V. The circuit was operated at $f_{\rm sw} = 100$ kHz in continuous conduction mode and the tests were carried out with the input voltage set to $V_{\rm IN} = 20$ V. Regarding the layout view of the test board, the primary loop is composed of the power transistor T, the free wheeling diode D and the decoupling capacitor $C_{\rm IN}$. It was laid out in order to meet common power circuit constraints and to host the secondary loop of the resonant transformer. Such a loop was designed in order to maximize the mutual coupling with the primary loop. Furthermore, the PCB hosts the pads at the primary loop (P1 in Fig. 6) and at the secondary loop (P2 in Fig. 6) needed for landing the RF probes to characterize the transformer with a vector network analyzer (VNA).

Finally, it is worst highlighting that the test board does not include any EMI input filter purposely, since the present research aims to highlight the real improvement resulting form the use of the proposed solution regardless of the EMI filter attenuation. A photograph of the fabricated test board highlighting the resonant snubber is shown in Fig. 5. About the passive components loading the secondary loop, R_2 and C_2, the values were obtained with the method presented in Section II. To that purpose, the free wheeling diode parasitic capacitance $C_{\rm D}$ (not shown in Fig. 6) and the transformer parameters, namely $L_{\rm P}$, $L_{\rm S}$ and M, were obtained by fitting the scattering parameters measured at the ports P1, P2 of the circuit comprising all the components except T and R_2. In that test, C_2 was replaced by a short circuit. The circuit was biased at the input by a DC voltage source $V_{\rm IN} = 20$ V, and SW was grounded through the VNA bias tee in order to keep the free wheeling diode D reverse biased, as it happens in the real circuit when the low side transistor T is switched on. A good matching between the measured scattering parameters and the simulated ones was obtained for $C_{\rm D} = 830$ pF, $L_{\rm P} = 17.4$ nH, $L_{\rm S} = 19.5$ nH, $M = 7.9$ nH. Therefore, $C_2 = 740$ pF and $R_2 = 2.2$ Ω were obtained from (5) and (8), respectively. Once the characterization of the transformer was completed, the power transistor was mounted on the test board and the circuit was operated without any snubber first, then with the resonant snubber loaded at the secondary with $C_2 = 740$ pF, $R_2 = 2.2$ Ω, and finally with the RC snubber ($R = 2.3$ Ω, $C = 3$ nF) connected in parallel to the free wheeling diode (the RC snubber is not shown in Fig. 6). The switching voltages to ground ($V_{\rm SW}$) at the turn on of the low side (T) measured with an oscilloscope, are shown in Fig. 7. The plots are limited to the falling edge since the rising one is much slower and it does not provide any useful information [7]. Such waveforms highlight that the oscillations causing the conducted emission peak are fully damped with the proposed snubbers as it is with conventional RC snubbers. The switching currents are not shown because the primary loop was laid out to control its stray inductance, therefore the shunt resistance was left out.

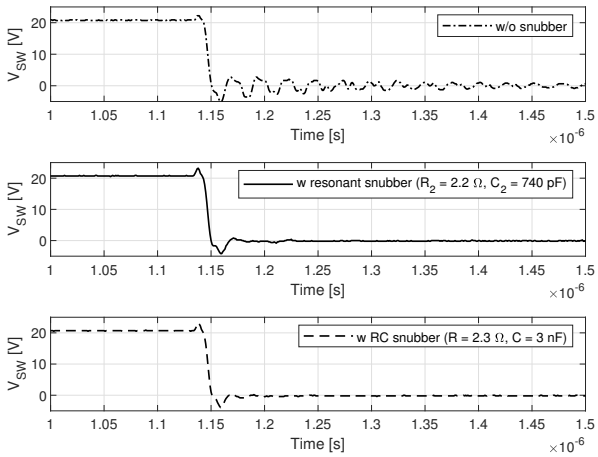

Fig. 7. SW voltage versus time measured without snubbers (dash-dotted line), with a tuned resonant snubber (continuous line), with a series RC snubber ($R = 2.3$ Ω, $C = 3$ nF) connected in parallel to the free wheeling diode (dashed line).

Aiming to check the reduction of the emission peaks the test board was inserted in a test bench compliant with CISPR 25 [11], which allows one to provide the device under test with the DC power supply through the Line Impedance Stabilization Networks (LISNs), which set the source impedance to

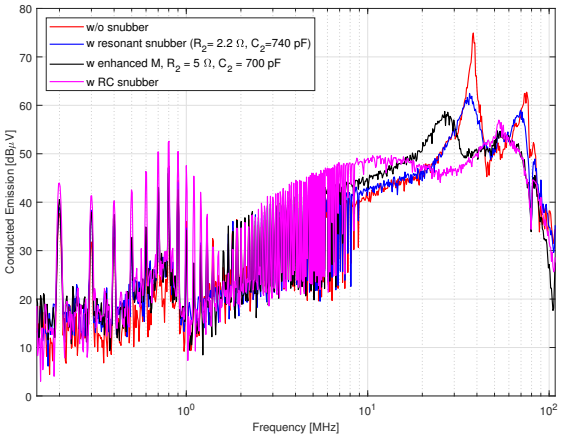

Fig. 8. Conducted emission spectra measured at the LISN RF port in accordance with CISPR 25. The results obtained without any snubber are shown in red, those with the proposed resonant snubber ($C_2 = 740$ pF, $R_2 = 2.2\Omega$) in blue, with the RC-snubber ($R = 2.3\ \Omega$, $C = 3$ nF) in magenta, with the resonant snubber having a better coupling between the primary and the secondary loop (ferrite rod, $C_2 = 700$ pF, $R_2 = 5\ \Omega$) in black.

ground to 50 Ω for each line from 150 kHz up to 108 MHz. The conducted emission measurements were repeated using the same test board but with different snubbers mounted on it. Fig. 8 shows the measurement results of the tested cases with different colours. The red curve was obtained without any snubber mounted on the prototype, meaning with the R_2 slot left open. The blue curve was obtained with the secondary loop loaded with $C_2 = 740$ pF and $R_2 = 2.2\ \Omega$ and the plot in magenta with the R_2 slot left open and a series RC snubber ($R = 2.3\ \Omega$, $C = 3$ nF) connected in parallel to the free wheeling diode. Finally, The measurement was repeated using the same test board but with an enhanced magnetic coupling between the two loops, which was obtained with a NiZn rectangular ferrite rod ($W = 8$ mm, $H = 6$ mm, $L = 8$ mm) inserted in the central PCB hole shown in the picture in Fig. 5. Also the transformer comprising the NiZn ferrite rod was characterized obtaining $L_P = 27.25$ nH, $L_S = 32.3$ nH, $M = 21.7$ nH, thus $C_2 = 700$ pF and $R_2 = 5\ \Omega$. The spectrum shown in black in Fig. 8 was obtained with the tiny ferrite rod inserted in the hole and with the above mentioned values for R_2 and C_2.

On balance, it can be concluded that the proposed solution attenuates the power loop resonance of about 15 dB (difference between the red and the blue spectra in Fig. 8) at about 40 MHz, which increases to about 18 dB if the coupling between the two loops is enhanced with a small ferrite rod. The considered RC snubber performs better up to 50 MHz to become similar to the proposed solution at higher frequencies. Finally, the energy dissipated by the proposed snubber (the case without the ferrite rod was considered) at each turn on of the low side transistor was evaluated on the basis of the voltage across R_2 and compared with that dissipated by the resistor R of the convetional RC snubber. From such measurements it came out that the energy dissipated in R_2 is $E_{R2} \simeq 200$ nJ ($R_2 = 2.2\ \Omega$, $C_2 = 740$ pF) and that dissipated in R is $E_R \simeq 1880$ nJ ($R = 2.3\ \Omega$, $C = 3$ nF). Specifically, each dissipated energy was evaluated referring to the falling edge of the switching voltage V_{SW}, since the rising edges were much slower, thus not able to trigger any oscillation.

IV. Conclusion

This work showed that the conducted emission peaks of the power switching circuits can be significantly attenuated using a resonant transformer integrated in the PCB hosting the power devices. A method to design such a resonant snubber was proposed and used in the design of a Buck converter. The circuit was prototyped and experimentally characterized performing conducted emission tests with the purpose of validating the proposed solution.

A maximum attenuation of the conducted emission peaks of about 15 dB at 40 MHz was observed with the air-core magnetic coupling, which increases to about 18 dB with the two loops coupled by a tiny ferrite core rod. Although the attenuation obtained with the resonant snubber is lower than that obtained with the RC snubber, the proposed solution shows lower power dissipation, since the resonant snubber is effective around the resonant frequency of the power loop only, whereas the capacitor of the RC snubber is charged and discharged at any commutation. Furthermore, given that the secondary loop is galvanically isolated from the power one, the circuit does not suffer from RC (RL) snubber reliability issues, and smaller components can be used.

References

[1] N. Oswald, P. Anthony, N. McNeill, and B. Stark, "An Experimental Investigation of the Tradeoff between Switching Losses and EMI Generation With Hard-Switched All-Si, Si-SiC, and All-SiC Device Combinations," IEEE Trans. on Pow. Electronics, vol. 29, no. 5, 2393-2407, May 2014.

[2] H.W. Ott, *Electromagnetic Compatibility Engineering*, Wiley, 2009.

[3] H. Park, S. Jeong, M. Kim, J. Kim, J. Jung, "Spread Spectrum Technique for Decreasing EM Noise in High Frequency APWM HB Resonant Converter with Reduced EMI Filter Size, " IEEE Trans. on Pow. Electronics, vol. 34, no. 11, 10845-10855, Nov. 2019.

[4] M. Perotti, F. Fiori, "A Closed Loop Delay Compensation Technique to Mitigate the Common Mode Conducted Emissions of Bipolar PWM Switched Circuits," IEEE Trans. on Pow. Electronics, vol. 36, no. 5, 5450-5459, June 2021.

[5] R.Erickson, D. Maksimovic, *Fundamentals of Power Electronics*, Kluwer Academic Publisher, 2001.

[6] L. Chen, H. Hu, Q. Zhang, A. Amirahmadi, I. Batarseh, "A Boundary-Mode Forward-Flyback Converter With an Efficient Active LC Snubber Circuit," IEEE Trans. on Pow. Electronics, vol. 33, no. 3, 2944-2958, June 2014.

[7] S. Lee, H. Choe, B Kang, "Quasi-Resonant Passive Snubber for Improving Power Conversion Efficiency of a DC–DC Step-Down Converter", IEEE Trans. on Pow. Electronics, vol. 29, no. 6, 2026-2034, Mar. 2018.

[8] Y. Xie, C. Chen, Z. Huang, T. Liu, Y. Kang, and F. Luo, "High frequency conducted EMI investigation on packaging and modulation for a SiC-based high frequency converter," IEEE J. Emerg. Sel. Topics Power Electron., vol. 7, no. 3, pp. 1789-1804, Sep. 2019.

[9] Y. Yano, N. Kawata, K. Iokibe, Y. Toyota, "A Method for Optimally Designing Snubber Circuits for Buck Converter Circuits to Damp LC Resonance", IEEE Trans. on Electromagn. Compat., vol. 61, no. 4, 1217-1225, Aug. 2019.

[10] R. Blecic, R. Gillon, B. N., A. Baric, "SPICE analysis of RL and RC snubber circuits for synchronous buck DC-DC converters", 38th Int. Convention on Information and Communication Technology, Electronics and Microelectronics (MIPRO), pp. 91-97, May 2015, Opatija, Croatia.

[11] "Vehicles, Boats and Internal Combustion Engines - Radio Disturbance Characteristics - Limits and Methods of Measurement for the Protection of On Board Receivers," IEC CISPR 25, 2008.